

RESEARCH ARTICLE

JMJD-1.2/PHF8 controls axon guidance by regulating Hedgehog-like signaling

Alba Redo Riveiro^{1,2,*‡}, Luca Mariani^{1,2,*‡}, Emily Malmberg^{1,2}, Pier Giorgio Amendola^{1,2}, Juhani Peltonen³, Garry Wong⁴ and Anna Elisabetta Salcini^{1,2,§}

ABSTRACT

Components of the KDM7 family of histone demethylases are implicated in neuronal development and one member, PHF8, is often found to be mutated in cases of X-linked mental retardation. However, how PHF8 regulates neurodevelopmental processes and contributes to the disease is still largely unknown. Here, we show that the catalytic activity of a PHF8 homolog in *Caenorhabditis elegans*, JMJD-1.2, is required non-cell-autonomously for proper axon guidance. Loss of JMJD-1.2 dysregulates transcription of the Hedgehog-related genes *wrt-8* and *grl-16*, the overexpression of which is sufficient to induce the axonal defects. Deficiency of either *wrt-8* or *grl-16*, or reduced expression of homologs of genes promoting Hedgehog signaling, restores correct axon guidance in *jmjd-1.2* mutants. Genetic and overexpression data indicate that Hedgehog-related genes act on axon guidance through actin remodelers. Thus, our study highlights a novel function of *jmjd-1.2* in axon guidance that might be relevant for the onset of X-linked mental retardation and provides compelling evidence of a conserved function of the Hedgehog pathway in *C. elegans* axon migration.

KEY WORDS: Epigenetics, Histone demethylase, Neuronal development, Axon guidance, Hedgehog signaling, *C. elegans*

INTRODUCTION

The KDM7 family of histone demethylases, which consists of three members, KDM7A (KIAA1718), KDM7B (PHF8) and KDM7C (PHF2), is characterized by the presence of a C-terminal JmjC domain and a PHD finger domain in the N-terminal portion. The members of this family have been associated with neurodevelopmental processes (Kleine-Kohlbrecher et al., 2010; Qiu et al., 2010; Qi et al., 2010; Tsukada et al., 2010; Huang et al., 2010) and deletions or mutations of PHF8 are often identified in cases of X-linked mental retardation (XLMR) (Siderius et al., 1999; Laumonier et al., 2005; Koivisto et al., 2007; Abidi et al., 2007; Loenarz et al., 2010; Redin et al., 2014), a highly heterogeneous group of inherited disorders characterized by impaired intellectual functions and cognitive abilities (Chiurazzi et al., 2004; Ropers and Hamel, 2005). While the JmjC domain of PHF8 catalyzes the

removal of H3K9me2/me1 and H4K20me1, its PHD finger binds H3K4me3 and contributes to the demethylase activity of the protein at appropriate target sites (Feng et al., 2010; Kleine-Kohlbrecher et al., 2010; Liu et al., 2010). Several studies have shown that PHF8 is required to control the expression of neuronal genes (Kleine-Kohlbrecher et al., 2010; Qiu et al., 2010; Fortschegger et al., 2010; Fortschegger and Shiekhattar, 2011); however, how PHF8 controls specific aspects of neuronal development and functions that may be relevant for the onset of the cognitive disorders remains poorly comprehended.

In mammals, the understanding of how specific factors orchestrate neurodevelopmental processes is challenged by the complexity of the nervous system, which consists of heterogeneous cellular populations comprising billions of neurons. The nematode *Caenorhabditis elegans* presents an excellent model to investigate these processes on a simpler and more tractable scale: its nervous system consists of 302 cells, whose morphology, function and connectivity have been extensively characterized (Sulston, 1983; White et al., 1986). Many chromatin regulators are conserved in *C. elegans* and important information regarding the role of these proteins in neuronal development has recently been obtained using this model system (Weinberg et al., 2013; Zheng et al., 2013; Mariani et al., 2016). PHF8 shares high homology with the *C. elegans* JMJD-1.2 protein, which retains both the JmjC and the PHD finger domains. However, the catalytic activity of JMJD-1.2 appears to differ from that of the mammalian counterpart, as several studies have shown its ability to demethylate not only H3K9me2, but also H3K27me2 and H3K23me2, both *in vitro* and *in vivo* (Kleine-Kohlbrecher et al., 2010; Lin et al., 2010; Vandamme et al., 2015). In agreement with the role of PHF8 in neuronal processes, JMJD-1.2 is required for normal locomotion in *C. elegans*, highlighting the importance of this protein in the establishment of neuronal functionalities (Kleine-Kohlbrecher et al., 2010).

During the development of the nervous system, a multitude of attractive and repulsive cues orchestrate the migration of neuronal cells and the direction of their processes (Ayala et al., 2007; Robichaux and Cowan, 2014). In addition to well-characterized ligands (such as netrins, slits, ephrins and semaphorins), a component of the Hedgehog family of morphogens, Sonic hedgehog, has been shown to regulate neural cell migration and axon guidance in vertebrates (Jarov et al., 2003; Bourikas et al., 2005; Sánchez-Camacho and Bovolenta, 2008; Hammond et al., 2009; Yam and Charron, 2013). Following synthesis and intracellular processing, Hedgehog (Hh) ligands are secreted by the combined action of receptors [i.e. Dispatched (DISP)], diffuse in the extracellular matrix through the interaction with lipoproteins and proteoglycans (LRP2 and Glypican 6) and target cells expressing Patched receptors (PTCH1/2). The binding of Hh to Patched activates the signaling pathway in receiving cells by releasing Smoothed (SMO) inhibition and triggering a signal transduction

¹Biotech Research & Innovation Centre (BRIC), University of Copenhagen, 2200, Copenhagen, Denmark. ²Centre for Epigenetics, University of Copenhagen, 2200, Copenhagen, Denmark. ³A. I. Virtanen Institute for Molecular Sciences, Department of Neurobiology, University of Eastern Finland, 70211, Kuopio, Finland. ⁴Faculty of Health Sciences, University of Macau, 999078, Macau, China.

*Present Address: The Danish Stem Cell Center (DanStem), University of Copenhagen, 2200, Copenhagen, Denmark.

‡These authors contributed equally to this work

§Author for correspondence (lisa.salcini@bric.ku.dk)

© A.E.S., 0000-0001-5828-2512

cascade through the regulation of Fused (FU) and Suppressor of fused (SUFU). Ultimately, this leads to the activation of Gli transcription factors, which control the expression of Hh target genes (Guerrero and Kornberg, 2014). Hh can also activate an alternative pathway (Jenkins, 2009) that is Gli- and, in some cases, SMO-independent, that leads to transcription-independent responses. Interestingly, this non-canonical Hh pathway regulates neural cell migration and axon guidance by modulating actin cytoskeleton reorganization (Bijlsma et al., 2007; Yam et al., 2009; Sasaki et al., 2010).

In the nematode, clear homologs of key components of the Hh pathway, including Hh, SMO, FU and SUFU have not been identified. Instead, the *C. elegans* genome encodes an abundance of what are collectively known as Hh-related proteins (WRT, GRL, GRD, QUA, HOG) based on their partial homology to domains found in the Hh proteins (Bürglin and Kuwabara, 2006; Kolotuev et al., 2009). Other molecules of this signaling pathway appear conserved in *C. elegans*, and homologs of factors required for Hh secretion (CHE-14, PTD-2/DISP), trafficking (GPN-1/Glypican 6, RIB-1/EXT1, RIB-2/EXTL3, LRP-1/LRP2, PHG-1/Gas1), Hh receptors (PTC-1, PTC-3/Patched) and transcription factors responsible for mediating Hh transcriptional activities (TRA-1/Gli1/3) have been identified. Ablation of some components of the Hh pathway results in defects in molting and body morphology (Zugasti et al., 2005; Hao et al., 2006a), suggesting that despite a considerable divergence some Hh functions are maintained in *C. elegans*.

Here, we show that the catalytic activity of JMJD-1.2 is required in the developing nervous system and hypodermis of *C. elegans* embryos to ensure correct axon guidance of specific neurons. Genome-wide analyses, in combination with genetic and overexpression studies, indicate that the defective axon guidance observed in *jmjd-1.2* mutants stems from the dysregulated transcription of a set of genes that includes two Hh-related molecules. Genetic analyses indicate that the axon guidance defects in *jmjd-1.2* mutant animals or that are caused by ectopic expression of Hh-related genes depend on actin remodelers, suggesting that the Hh-like pathway controls axon guidance by regulating actin dynamics.

RESULTS

jmjd-1.2 mutants display neuronal defects

To gain insight into the role of JMJD-1.2 in the nervous system, we analyzed different axon guidance and neuronal cell migration events in the *jmjd-1.2* mutant allele *tm3713*, which carries an in-frame deletion that removes the region encoding the PHD finger domain (Kleine-Kohlbrecher et al., 2010; Lin et al., 2010). Although transcribed (Kleine-Kohlbrecher et al., 2010), the deleted locus results in loss of the JMJD-1.2 protein, as we and others could not detect JMJD-1.2 by western blot or immunofluorescence, suggesting that *tm3713* is probably a null mutant (Fig. 1A,B) (Lin et al., 2010). Using a specific antibody, JMJD-1.2 appears expressed in many, if not all, nuclei (Fig. 1B, Fig. S1A), confirming the expression pattern identified analyzing the

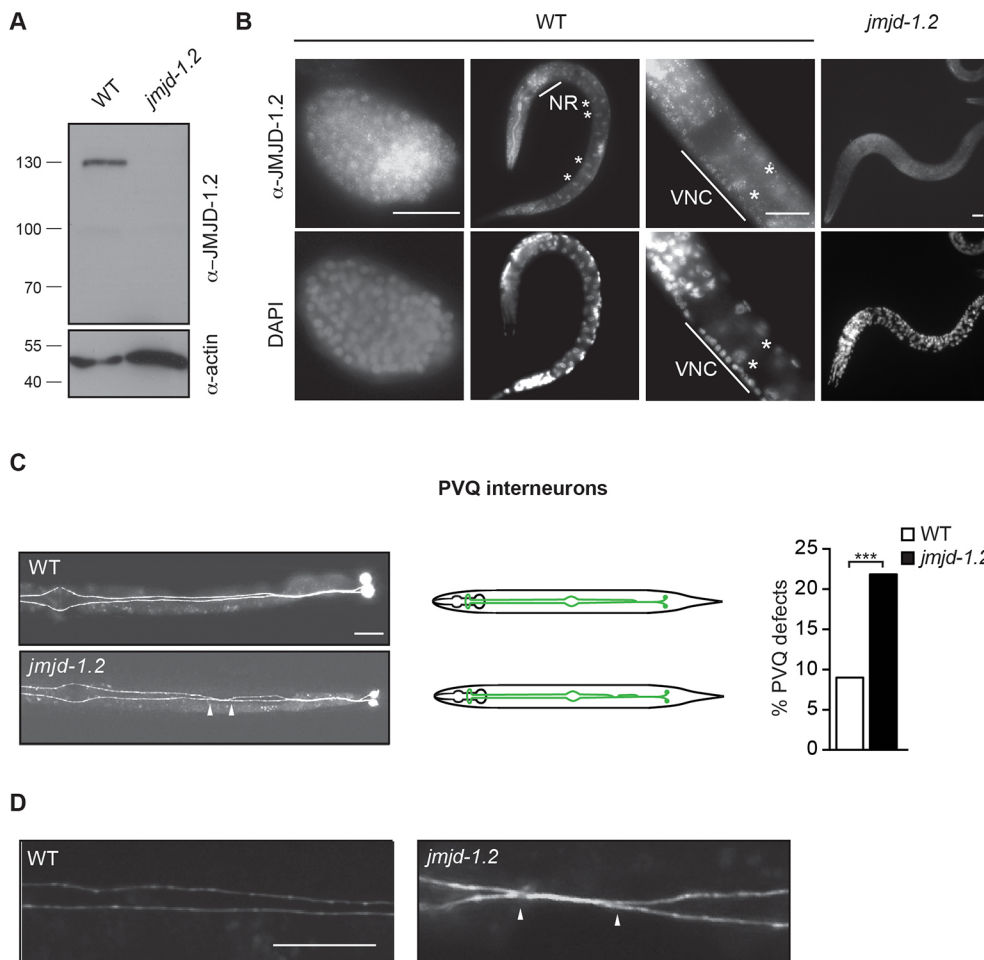


Fig. 1. JMJD-1.2 is required for correct axon guidance. (A) Wild-type (WT) and *jmjd-1.2(tm3713)* whole-worm lysates assayed by immunoblotting with JMJD-1.2 antibody. Actin is used as loading control. Size standards are kDa. (B) Representative images of wild-type and *jmjd-1.2(tm3713)* animals, fixed and stained with JMJD-1.2 antibody. DNA was counterstained with DAPI. Asterisks indicate intestinal cells and the lines indicate neurons of the nerve ring (NR) or ventral nerve cord (VNC). (C) (Left) Representative images of PVQ neurons in wild-type and *jmjd-1.2(tm3713)* adult animals, visualized using the transgene *oyIs14*. (Middle) Schematics of PVQ neurons in wild-type and *jmjd-1.2(tm3713)* animals. (Right) Quantification of PVQ axonal crossover defects in *jmjd-1.2(tm3713)* animals. $n > 200$; *** $P < 0.001$ (Fisher's exact test). (D) High-magnification image of PVQ axons in wild-type and *jmjd-1.2(tm3713)* adult animals, visualized using the transgene *oyIs14*. Arrowheads (C,D) indicate the points of axonal crossover. Ventral views, anterior to the left. Scale bars: 20 μ m.

expression of a GFP-tagged JMJD-1.2 construct (Kleine-Kohlbrecher et al., 2010).

Using transgenic animals carrying fluorescent markers for specific neurons, we found that loss of JMJD-1.2 led to the aberrant migration of axons projected by specific pairs of neurons, namely PVQs and HSNs. In wild-type animals, PVQ cellular bodies are located in the lumbar ganglia and their projections run along two distinct bundles of the ventral nerve cord. In *jmjd-1.2(tm3713)* mutant animals, PVQ neurons are born and positioned correctly, but their axons fail to maintain the correct trajectory and aberrantly cross over the ventral midline in 22% of the population (Fig. 1C,D). A similar phenotype was identified in a null mutant generated by the CRISPR/Cas9 system (Fig. S1B). Axonal defects were also observed in the HSN neurons (Table 1, Fig. S1C,D). Occasionally, the HSN cellular bodies, which are normally located in the vulva region, undermigrated, suggesting an additional role for *jmjd-1.2* in neuronal cell body positioning. Moreover, in *jmjd-1.2(tm3713)* mutants, the expression of the *evls82b* transgene, which is specifically expressed in DA/DB motoneurons, was often reduced in the body and projection of DB5 (Table 1, Fig. S1E,F). Transgenic animals carrying constructs expressed in other neurons, however, showed normal patterning of axon migration (Table 1), suggesting that loss of *jmjd-1.2* does not affect the whole architecture of the nervous system.

JMJD-1.2 acts during embryogenesis in nervous system and hypodermis to ensure correct axon guidance

To study the function of JMJD-1.2 in axon guidance, we focused on the analysis of the PVQs, well-studied interneurons that fully

develop during embryogenesis. To test whether the PVQ axonal defects observed in *jmjd-1.2* mutants occur in embryogenesis or during larval development, we analyzed the PVQ neurons of freshly hatched L1 mutant larvae. As shown in Fig. 2A, the penetrance of the phenotype at this stage was comparable to that of L4 animals, suggesting that the defects arise during embryonic development and are not related to defective maintenance of axon pathfinding (Aurelio et al., 2002; Pocock et al., 2008; Bénard et al., 2012).

Transgenic expression of a translational fusion between the *jmjd-1.2* genetic locus and *GFP* could rescue the PVQ defects observed

Table 1. Summary of phenotypes in *jmjd-1.2(tm3713)* mutants

Neurons examined (marker used)	Defective animals (%)		P-value
	WT	<i>jmjd-1.2(tm3713)</i>	
Head neurons			
Amphid neurons* (Dil)	0	0	
VNC neurons			
Interneurons			
AVK interneurons [‡] (<i>bwls2</i>)	0	3	
AVG interneuron [‡] (<i>otls182</i>)	0	0	
PVP interneurons [‡] (<i>hdls26</i>)	9	20	P<0.01
PVQ interneurons [‡] (<i>oyls14</i>)	9	22	P<0.001
Motoneurons			
HSN motoneurons (<i>zdl13</i>)			
Axon guidance [‡]	6	36	P<0.001
Cell migration [§]	5	34	P<0.001
D-type motoneurons (<i>oxls12</i>)			
Midline left/right choice [¶]	31	50	
DA/DB motoneurons (<i>evls82b</i>)			
Midline left/right choice [¶]	4	4	
Transgene expression reduced in DB5 [#]	2	32	P<0.001
DVB motoneuron ^{**} (<i>oxls12</i>)	0	0	
Sensory neurons			
PDE neurons ^{**} (<i>qls2</i>)	5	9	
Tail neurons			
Phasmid neurons* (Dil)	0	0	

Neurons were examined using the indicated transgenic markers and the diffusible dye Dil. Statistical significance of the difference between wild type and mutants was assessed with Fisher's exact test. $n>100$. Animals were considered defective if: *neurons were not stained with Dil; †axons crossed over the VNC; ‡neuronal cells were misplaced; ¶the commissure of at least one motoneuron extended on the wrong side of the body; #transgene expression was reduced in DB5; **transgene expression was absent in DVB; ††axons failed to reach the VNC.

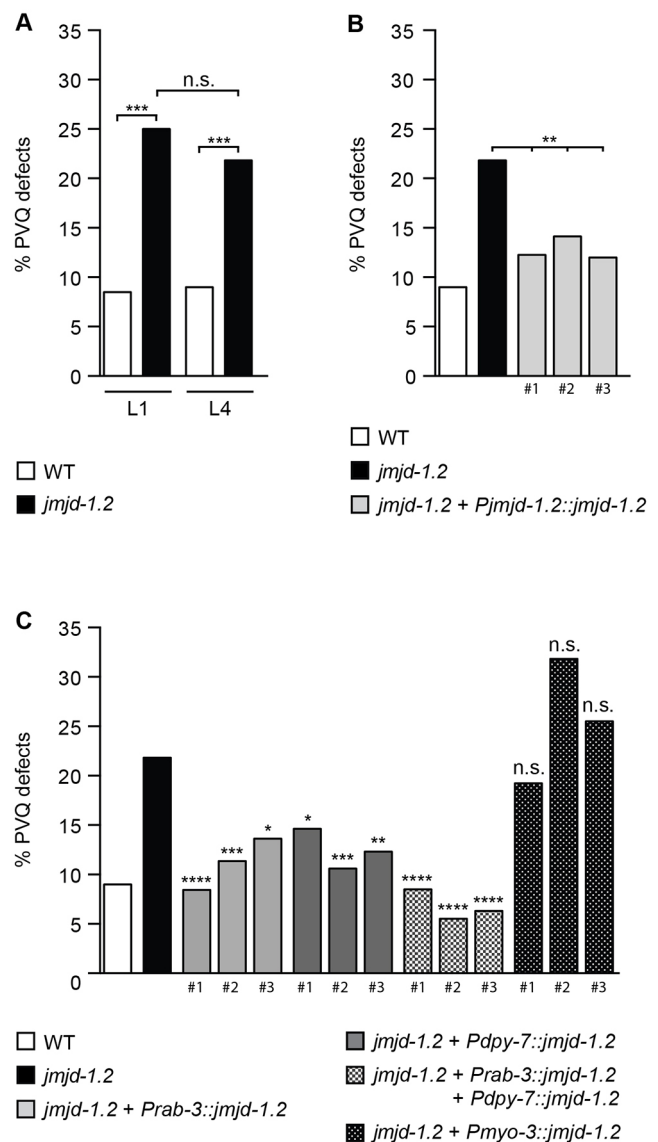


Fig. 2. JMJD-1.2 acts during embryogenesis in both nervous system and hypodermis to ensure correct axon guidance. (A) Quantification of PVQ axonal crossover defects in *jmjd-1.2(tm3713)* mutants at L1 and L4 stages. $n>100$. (B) Rescue of PVQ axonal crossover defects in *jmjd-1.2(tm3713)* expressing the *Pjmjd-1.2::jmjd-1.2::GFP* translational reporter. (C) Tissue-specific rescue analyses. Promoters used for transgenic rescue are: *Prab-3*, nervous system; *Pdp-7*, hypodermis; *Pmyo-3*, muscle cells. (B,C) Statistical significance was calculated in relation to non-transgenic controls (values not shown) for each transgenic line. $n>100$. (A-C) * $P<0.05$, ** $P<0.01$, *** $P<0.001$, **** $P<0.0001$; n.s., not significant (one-way ANOVA followed by Tukey's multiple-comparison test). Three independent lines for each transgene (indicated by #) were analyzed.

in *tm3713*, confirming that the axon guidance phenotype is due to loss of JMJD-1.2 (Fig. 2B, Table S1). Previous studies have shown that *jmjd-1.2* is expressed at all developmental stages and in multiple tissues, including neurons, muscles, intestine and hypodermis (Kleine-Kohlbrecher et al., 2010), a spatiotemporal expression confirmed by immunostaining with a specific antibody (Fig. 1B). To uncover the focus of action of JMJD-1.2 in the context of PVQ axon guidance, we re-expressed GFP-tagged JMJD-1.2 in the *tm3713* background using a panel of tissue-specific promoters (Fig. 2C, Fig. S2, Table S1). We drove *jmjd-1.2* expression under the control of either *rab-3* (nervous system) or *dpy-7* (hypodermis) promoters and found significant rescue of PVQ defects in each case, although the rescue effect was slightly enhanced by re-expressing JMJD-1.2 in both tissues simultaneously (Fig. 2C). By contrast, we could not rescue the phenotype by expressing *jmjd-1.2* under the *myo-3* (body wall muscle) promoter, showing that the presence of JMJD-1.2 in muscle cells is not required for axon guidance (Fig. 2C). In agreement with the requirement of JMJD-1.2 in multiple tissues, driving its expression in the PVQ or in the pioneer PVP neurons was not sufficient to restore the normal guidance of PVQs, suggesting that JMJD-1.2 does not work cell-autonomously nor in PVPs (Fig. S3). Altogether, these data strongly suggest that JMJD-1.2 controls the guidance of PVQs in both nervous system and hypodermis.

The JmjC and PHD finger domains of JMJD-1.2 are essential for correct axon guidance

JMJD-1.2 is structured around two evolutionarily conserved domains: the JmjC domain and the H3K4me3-binding PHD finger (Kleine-Kohlbrecher et al., 2010; Lin et al., 2010). The JmjC domain of JMJD-1.2 has been shown to demethylate H3K9me2, H3K27me2 and H3K23me2 *in vitro* and *in vivo* and, accordingly, increased signal of these post-translational modifications is found in the *tm3713* mutant strain (Kleine-Kohlbrecher et al., 2010; Lin et al., 2010; Vandamme et al., 2015). To test the relevance of JMJD-1.2 enzymatic activity in axon guidance, we mutated the JmjC domain (Fig. 3A) by substituting two conserved amino acids required for the catalytic activity (Klose et al., 2006; Kleine-Kohlbrecher et al., 2010), and performed rescue experiments by re-expressing the inactive form of JMJD-1.2 (JMJD-1.2_JmjCmut) in the *tm3713* background. Whereas wild-type JMJD-1.2 could restore normal PVQ guidance, the mutated protein could not (Fig. 3B, Table S1), revealing the essential role of JMJD-1.2 catalytic activity in axon guidance. Interestingly, mutations affecting the demethylase activity of the human homolog PHF8 are linked to neurological disorders (Koivisto et al., 2007; Loenarz et al., 2010; Qiu et al., 2010). Among others, the missense mutation c.836C>T encodes an F279S variant of the protein that is associated with mild XLMR and dysmorphic features (Koivisto et al., 2007). This mutation resides in the JmjC domain and has been shown to disrupt the catalytic activity of the protein (Loenarz et al., 2010; Qiu et al., 2010). As the region is highly conserved in *C. elegans*, we were able to generate a version of JMJD-1.2 bearing a similar mutation (JMJD-1.2_XLMR, Fig. 3A). When re-expressed in the *tm3713* background, this mutant protein did not rescue PVQ axon guidance defects (Fig. 3B, Table S1).

Besides the JmjC domain, JMJD-1.2 carries a PHD finger that, as in the mammalian counterpart, has been shown to mediate binding to H3K4me3 and to contribute to demethylase activity both *in vitro* and *in vivo* (Lin et al., 2010). To assess the role of this domain in axon guidance, we generated a mutation in a specific residue that is important for the binding to H3K4me3 and for the catalytic activity

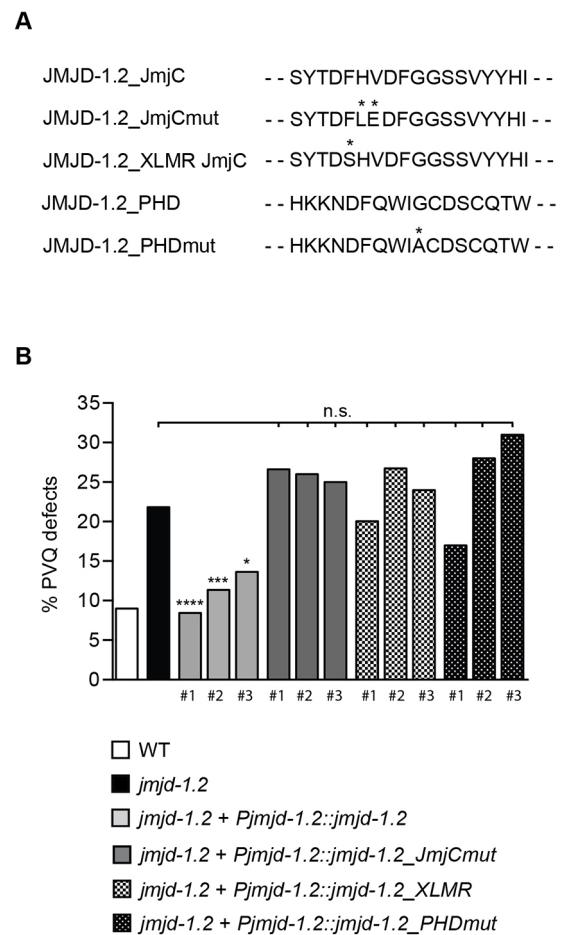


Fig. 3. The JmjC and PHD finger domains of JMJD-1.2 are required for correct axon guidance. (A) Amino acid sequences from the JmjC and PHD finger domains of wild-type JMJD-1.2 and of the catalytically inactive derivative (JMJD-1.2_JmjCmut), that bearing a mutation associated with X-linked mental retardation (JMJD-1.2_XLMR) and that with a mutated PHD finger (JMJD-1.2_PHDmut); changes are marked with an asterisk. (B) Quantification of PVQ axonal crossover defects in *jmjd-1.2(tm3713)* animals expressing the indicated translational constructs. Statistical significance was calculated in relation to non-transgenic controls (values not shown) for each transgenic line. $n > 100$; * $P < 0.05$, *** $P < 0.001$, **** $P < 0.0001$; n.s., not significant (one-way ANOVA followed by Tukey's multiple-comparison test). Three independent lines for each transgene (indicated by #) were analyzed.

of JMJD-1.2 (Lin et al., 2010; Yang et al., 2010). As with the catalytically inactive protein, the enzyme bearing a mutated PHD finger (JMJD-1.2_PHDmut, Fig. 3A) was unable to restore correct axon guidance (Fig. 3B, Table S1).

Altogether, these data show that the JmjC domain and the PHD finger are both required to correctly drive the process of axon guidance and indicate that the demethylase activity and ability of JMJD-1.2 to bind H3K4me3 are essential in this context.

jmjd-1.2-associated defects depend on dysregulated transcription

Previously, it was reported that loss of JMJD-1.2 is associated with dysregulated gene transcription (Lin et al., 2010). As *jmjd-1.2* activity is important during embryogenesis, we analyzed the transcriptome of *jmjd-1.2(tm3713)* mutant embryos by RNA sequencing (RNA-seq). Notably, only 22 genes displayed expression changes of more than 1.5-fold between wild type and mutants, of which 16 could be further validated by qPCR (Table 2).

Table 2. Genes with dysregulated expression in *jmjd-1.2(tm3713)* mutants

Gene	Fold change	qPCR	Allele	Functions
<i>C38D9.2</i>	5.81	No		n.d.
<i>wrt-8</i>	4.08	Yes	<i>tm1585</i>	Hh-like protein
<i>F15E6.10</i>	3.68	Yes		n.d.
<i>clec-230</i>	3.13	Yes	<i>ok3131</i>	C-type lectin
<i>asp-6</i>	2.05	Yes	<i>tm2213</i>	Predicted protease
<i>grl-7</i>	2.05	Yes	<i>ok2644</i>	Hh-like protein
<i>C02E7.7</i>	1.99	No		n.d.
<i>C08B6.4</i>	1.91	Yes		Predicted chitinase activity
<i>F10D11.6</i>	1.90	Yes		Predicted lipid binding
<i>grl-16</i>	1.89	Yes	<i>ok2959</i>	Hh-like protein
<i>asp-1</i>	1.87	Yes		Predicted protease
<i>lgc-22</i>	1.83	Yes		Ligand-gated ion channel
<i>ZK180.5</i>	1.82	Yes		n.d.
<i>bcl-11</i>	1.81	Yes		Homology to BCL11A
<i>Y47D7A.13</i>	1.79	n.t.		n.d.
<i>nep-17</i>	1.77	Yes	<i>ok3251</i>	Predicted metalloproteinase
<i>cut-3</i>	1.72	Yes	<i>ok1819</i>	Cuticlin
<i>F41F3.3</i>	1.71	n.t.		n.d.
<i>cut-2</i>	1.62	Yes		Cuticlin
<i>drd-2</i>	1.62	Yes		Homology to TENM3
<i>hsp-16.41</i>	-2.0	No		Heat shock protein
<i>hsp-16.11</i>	-2.2	No		Heat shock protein

List of genes found to be dysregulated by RNA-seq in *jmjd-1.2(tm3713)* compared with wild-type embryos. A filter of 1.5-fold difference and FDR correction ($P < 0.05$) were applied. Validation by qPCR, available mutant alleles and gene functions are indicated; n.d., not determined; n.t., not tested.

All validated genes are significantly upregulated in this allele (Table 2, Fig. S4). We speculated that, if the overexpression of these genes was responsible for *jmjd-1.2* axon guidance defects, their removal from the *tm3713* background could ameliorate the axonal phenotype. As viable mutants for some of these genes are available, we generated double mutants with *jmjd-1.2* and analyzed them for PVQ defects. Loss of either *clec-230*, *cut-3*, *wrt-8* or *grl-16* restored correct PVQ guidance (Fig. 4A, Table S2). Interestingly, both *wrt-8* and *grl-16* encode Hh-related proteins (Aspöck et al., 1999; Hao et al., 2006b), raising the possibility that *C. elegans* Hh signaling, similar to the vertebrate counterpart, might play a key role in axon guidance. To strengthen this hypothesis, we tested whether overexpression of *wrt-8* or *grl-16* in wild-type embryos could reproduce the PVQ guidance defects observed in *jmjd-1.2* mutants. As we were unable to obtain transgenic lines continuously overexpressing these proteins, we generated animals that carry heat shock-inducible *wrt-8* or *grl-16* genomic regions, using the *hsp-16.2* promoter. Strikingly, when *wrt-8* or *grl-16* expression was transiently induced during embryogenesis, we observed PVQ axon defects that were similar to those associated with loss of JMJD-1.2, both qualitatively and quantitatively (Fig. 4B–D). Importantly, this effect was not observed when the expression was forced at later developmental stages, for example in L1, providing an important internal control and supporting the role of *jmjd-1.2* in regulating the expression of *wrt-8* or *grl-16* in embryos.

***jmjd-1.2* axonal defects depend on Hh signaling**

Although the Hh pathway has undergone a prominent divergence during evolution, some key molecules of the canonical Hh signaling are conserved in *C. elegans* (Bürglin and Kuwabara, 2006; Kolotuev et al., 2009) (Table S3) and are involved in the trafficking of proteins and sterols, similar to the vertebrate

counterparts (Kuwabara et al., 2000; Hao et al., 2006b; Soloviev et al., 2011). As the defects observed in *jmjd-1.2* mutants are related to increased expression of Hh-related genes, we speculated that a negative regulation of the Hh pathway could ameliorate the *jmjd-1.2* phenotype. Homologs of genes required for Hh release (*DISP/che-14*) and propagation of the signal (*Glypican 6/gpn-1*, *EXT1/rib-1* or *EXTL3/rib-2*) have been identified in *C. elegans*. We analyzed the effect of reduction by RNA interference (RNAi) or depletion (using mutants when available) of these conserved genes in the *jmjd-1.2* background and invariably observed a significant amelioration of the *jmjd-1.2* axon guidance phenotype (Table 3). Similarly, we predicted that reduction of Hh-like receptors and co-receptors (Patched/PTC-1/PTC-3, Megalin/LRP2/LRP-1, Gas1/PHG-1) could also influence the *jmjd-1.2* phenotype. Strikingly, reduction of *lrp-1*, *phg-1* and *ptc-1*, but not *ptc-3*, in *jmjd-1.2* mutants also resulted in significant amelioration of the phenotype, further supporting a causal role of dysregulated Hh signaling in the defective axon guidance of the *jmjd-1.2* mutant (Table 3). By contrast, reduction of homologs of *skn/hhat-1/hhat-2*, required for palmitoylation of Hh, failed to significantly ameliorate the phenotype, similar to the ablation of *grl-7*, another Hh-related protein that was upregulated in our RNA-seq data. Overall, the genetic ablation or reduction by RNAi of several conserved components of the Hh pathway from the *tm3713* background is sufficient to rescue the PVQ defects associated with loss of *jmjd-1.2*. That the defects observed in *jmjd-1.2* mutants can be rescued by its ectopic expression in hypodermis or neurons suggests that the components of the Hh pathway might be dysregulated in multiple tissues and that the re-expression of *jmjd-1.2* in hypodermis or neuron is sufficient to restore a correct level of Hh signaling and therefore proper axon guidance.

Altogether, these findings strongly suggest that aberrant activation of Hh signaling is responsible for the defects observed in *jmjd-1.2* mutants. Furthermore, our data provide the first evidence that some evolutionarily conserved proteins of the Hh signaling pathway act in axon guidance in *C. elegans*.

Implication of actin dynamics in *jmjd-1.2* defects

Many studies in several model organisms, including *C. elegans*, indicate that axon growth and guidance are ultimately regulated by actin cytoskeleton remodeling at growth cones (Kalil and Dent, 2005; Quinn and Wadsworth, 2008; Dent et al., 2011; Chia et al., 2014; Gomez and Letourneau, 2014). We therefore postulated that JMJD-1.2 might regulate actin dynamics and tested this by systematically ablating several conserved actin regulators in the *jmjd-1.2* genetic background and further analyzing the axon migration of PVQ neurons. We generated double mutants carrying the *jmjd-1.2* deletion together with mutations in well-established actin regulator genes such as *wsp-1/WASP*, *wve-1/WAVE*, *unc-34/Ena/VASP*, *cdc-42/CDC42*, *mig-2/RAC*, *nck-1/NCK* and *wip-1/WIP*. Whereas the removal of *wve-1*, *mig-2*, *unc-34* or *cdc-42* was ineffective, loss of *wsp-1* and its regulators *wip-1* and *nck-1* resulted in a significant rescue of the *jmjd-1.2* phenotype (Fig. 4E), strongly suggesting that the *jmjd-1.2* axonal defects depend on aberrant actin remodeling mediated by *wsp-1*. Of note, none of the actin regulators is apparently dysregulated at the transcriptional level in *jmjd-1.2* mutant animals, as indicated by RNA-seq analysis, suggesting that Hh signaling in *C. elegans* might regulate axon migration in a transcription-independent manner. Importantly, overexpression of *grl-16* or *wrt-8* in a *wsp-1* mutant background was unable to induce PVQ axon guidance defects, suggesting that the axonal defects of *jmjd-1.2* mutants depend on

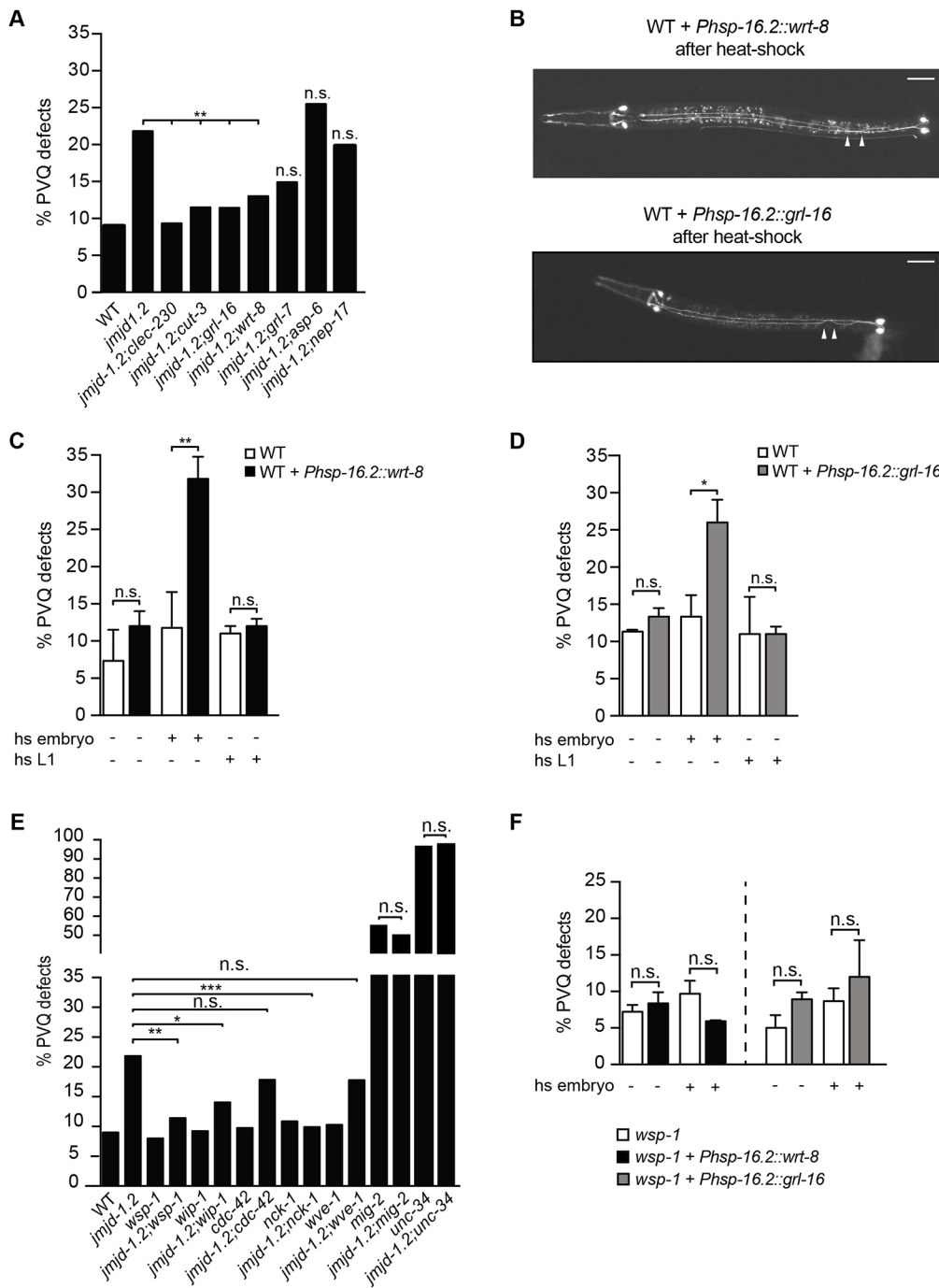


Fig. 4. Axon guidance defects resulting from overexpression of Hh-like proteins are mediated by actin remodeling. (A) Quantification of PVQ axonal crossover defects in the indicated strains. $n > 100$. (B) Representative images of wild-type young larvae carrying translational constructs for WRT-8 or GRL-16 under the control of a heat shock (*Phsp-16.2*) promoter, after heat shock at embryonic stage. PVQ neurons are visualized using the *oyIs14* transgene. Arrowheads indicate the points of axonal crossover. Ventral view, anterior to the left. Scale bars: 20 μ m. (C,D) Quantification of PVQ axonal crossover defects in wild-type animals carrying translational constructs for WRT-8 (B) and GRL-16 (C) expressed under the control of the *Phsp-16.2* promoter, before and after heat shock at embryonic or L1 larval stages. $n > 100$. (E) Quantification of PVQ axonal crossover defects in the indicated strains. $n > 150$. (F) Quantification of PVQ axonal crossover defects in *wsp-1* (*gm324*) mutants carrying translational constructs for WRT-8 or GRL-16 expressed under the control of the *Phsp-16.2* promoter, before and after heat shock at embryonic stages. $n > 150$. (A,C-F) $*P < 0.05$, $**P < 0.01$, $***P < 0.001$; n.s., not significant (one-way ANOVA followed by Tukey's multiple-comparison test). (C,D,F) Results are from three independent experiments and error bars represent s.e.

Hh-mediated actin regulation (Fig. 4F). This hypothesis is in agreement with previous studies reporting that Hh triggers a transcription-independent signaling cascade that acts rapidly and locally at the growth cone to regulate actin-based structure dynamics and axon migration (Charron and Tessier-Lavigne, 2005; Bijlsma et al., 2007; Yam et al., 2009; Sasaki et al., 2010). Altogether, these experiments suggest that *jmjd-1.2* regulates Hh signaling and actin reorganization at the growth cone of migrating neurons.

DISCUSSION

In this study, we have found that *jmjd-1.2* regulates some aspects of neuronal development, including axon guidance (PVQs and HSNs) and neuronal cell body migration (HSNs). As the axon migration in PVQs and HSNs occurs during embryonic and larval

stages, respectively, these results suggest a regulatory role for *jmjd-1.2* across development. We have also observed reduced expression of the transgene *evIs82b*, carrying the terminal selector gene *unc-129*, in the DB5 motoneuron, supporting a function of *jmjd-1.2* in the process of neuronal differentiation. Interestingly, this deficiency might contribute to the locomotion defects previously described in *jmjd-1.2* mutants (Kleine-Kohlbrecher et al., 2010).

Notably, the catalytic activity of JMJD-1.2 is fundamental to ensure correct axon guidance. Given that this demethylase is able to remove the dimethyl mark from different lysine residues on histone H3, we cannot, at the moment, link the observed neuronal defects to a specific activity of JMJD-1.2 on one or more residues. In addition, our results indicate that the correct recruitment of JMJD-1.2 to

Table 3. Loss or reduction of distinct members of the Hh family rescues PVQ defects in *jmjd-1.2(tm3713)* mutants

Genotype	Rescue	Defective animals (%)	<i>n</i>	<i>P</i> -value
WT		9	>400	
<i>jmjd-1.2(tm3713)</i>		22	>400	
<i>jmjd-1.2(tm3713);gpn-1(ok377)</i>	Yes	12	221	0.0186*
<i>jmjd-1.2(tm3713);che-14(e1960)</i>	Yes	13	191	0.0269*
<i>jmjd-1.2(tm3713);che-14(ok193)</i>	Yes	11	178	0.0023*
WT+RNAi control		5	346	
<i>jmjd-1.2(tm3713)+RNAi control</i>		14	384	0.0002 [§]
<i>jmjd-1.2(tm3713)+lrp-1 RNAi</i>	Yes	8	474	0.0149 [‡]
<i>jmjd-1.2(tm3713)+ptc-1 RNAi</i>	Yes	8	235	0.0334 [‡]
<i>jmjd-1.2(tm3713)+ptc-3 RNAi</i>	No	13	332	1.000 [‡]
<i>jmjd-1.2(tm3713)+rib-1 RNAi</i>	Yes	8	275	0.0344 [‡]
<i>jmjd-1.2(tm3713)+rib-2 RNAi</i>	Yes	8	294	0.0496 [‡]
<i>jmjd-1.2(tm3713)+hhhat-1 RNAi</i>	No	13	216	1.000 [‡]
<i>jmjd-1.2(tm3713)+hhhat-2 RNAi</i>	No	11	252	0.3467 [‡]
<i>jmjd-1.2(tm3713)+tra-1 RNAi</i>	No	16	504	0.2390 [‡]

Statistical significance (compared with **jmjd-1.2(tm3713)*, †*jmjd-1.2(tm3713)+RNAi control* or §WT+RNAi control) was assessed by one-way ANOVA followed by Tukey's multiple-comparison test. *n*, number of animals analyzed.

chromatin, mediated by the PHD domain, is similarly important. It has been shown previously that JMJD-1.2 and its mammalian homolog PHF8 are recruited to promoters, where they control gene expression (Lin et al., 2010; Kleine-Kohlbrecher et al., 2010; Fortschegger et al., 2010). By RNA-seq, we identified minor changes in the transcriptome of *jmjd-1.2* mutant embryos compared with wild type, and the few genes that were perturbed were

upregulated. Although the low number of dysregulated genes detected could be related to the experimental setting (we used mixed populations of embryos, which could have hidden tissue- and stage-specific changes in gene expression), the upregulation of gene transcription in association with increased levels of H3K9/K27/K23me2, which are marks that have been generally linked to gene repression, is unexpected and suggests that the dysregulated genes might be indirect targets of JMJD-1.2.

Among the upregulated genes, we identified those encoding the Hh-related proteins WRT-8 and GRL-16, and showed that their transient overexpression in wild-type embryos induces axon guidance defects similar to those identified in *jmjd-1.2* mutant animals. This strongly suggests that dysregulation of *wrt-8* and *grl-16* is causal for the *jmjd-1.2* axonal phenotype. Further, we have shown that loss or reduction of genes encoding homologs of components of the Hh pathway, including *wrt-8* and *grl-16*, is sufficient to rescue the *jmjd-1.2* defects. These results support a previously unappreciated role of Hh-like signaling in axon guidance in *C. elegans*. Two other genes were found to be upregulated in *jmjd-1.2* mutant animals, and their loss was sufficient to restore normal axon guidance in *jmjd-1.2* mutants: *clec-230*, which encodes a protein of 179 amino acids that contains a lectin domain, a carbohydrate-binding module often found in proteins with functions in adhesion (Drickamer and Dodd, 1999); and *cut-3*, which encodes a component of the worm cuticle and is specifically expressed in the embryo (Sapio et al., 2005). Neither *cut-3* nor *clec-230* has clear homologs in mammals and they were not investigated further. Although it is possible that these genes are Hh transcriptional target genes, it is also conceivable that, being molecules implicated in adhesion and extracellular matrix composition, they could play a role in Hh diffusion.

The role of the Hh pathway in axon guidance remains poorly understood, but some studies indicate that in this context Hh triggers an alternative, transcription-independent signaling cascade that acts rapidly and locally at the growth cone to induce actin cytoskeleton remodeling (Charron and Tessier-Lavigne, 2005; Bijlsma et al., 2007; Yam et al., 2009; Sasaki et al., 2010). Interestingly, our genetic interaction analyses suggest that molecules regulating actin dynamics play a role in the establishment of aberrant axonal migration in *jmjd-1.2* mutants. In support of this, it has previously been reported that downregulation of PHF8 results in cytoskeleton disorganization and in cell adhesion defects (Asensio-Juan et al., 2012). It is possible that altered actin dynamics counteract the effects of increased Hh signaling by regulating Hh trafficking and secretion. However, based on our previous findings that misexpression of actin regulators in PVQ neurons causes aberrant axon guidance (Mariani et al., 2016) and on our overexpression experiments in the *wsp-1* mutant background, we favor a hypothesis (Fig. 5) in which JMJD-1.2 modulates the expression of Hh-related proteins in neuronal and hypodermal cells, which, after secretion, activate a signaling pathway controlling actin remodeling and axon guidance in target neurons. How dysregulation of the Hh pathway impacts actin dynamics, thereby leading to incorrect axon guidance, is a key aspect that remains to be investigated. As we did not identify any transcriptional dysregulation of actin regulators in *jmjd-1.2* mutants by RNA-seq, it is tempting to speculate that JMJD-1.2 might modulate the activity and/or cellular localization of actin regulators. Similarly, the tissue specificity of Hh signaling components remains unknown and further analyses will be required to identify not only the specific cells secreting the ligands (signaling cells) but also those expressing Hh receptors (receiving cells). Theoretically, despite being obtained in

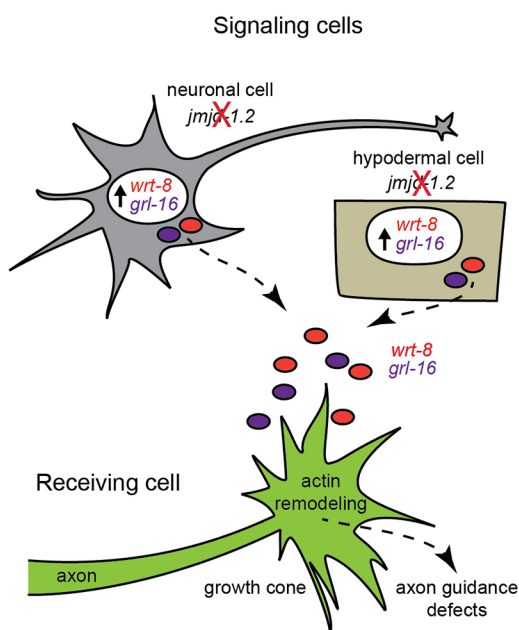


Fig. 5. Model of JMJD-1.2 action as a negative transcriptional regulator of Hh-related genes *wrt-8* and *grl-16*. Upon loss of *jmjd-1.2*, unidentified hypodermal cells and neurons (signaling cells) secrete abnormally high levels of WRT-8 and GRL-16, causing axon guidance defects in receiving cells (e.g. PVQs) by impairing proper actin cytoskeleton remodeling at the growth cone.

C. elegans, our results suggest that an aberrant Hh pathway could be related to XLMR and other cognitive diseases, such as intellectual disability (ID) or autism spectrum disorder (ASD). Supporting this possibility, the Hh acyltransferase HHAT has been identified as mutated in whole-exon sequencing and proposed as a candidate gene for ID (Agha et al., 2014). Similarly, PTCHD1, which shares high homology with the Patched receptors, has been suggested as a candidate gene for ASD and ID (Noor et al., 2010; Filges et al., 2011; Chaudhry et al., 2015).

We recently identified RBR-2, an H3K4me3/2 histone demethylase, as being implicated in the regulation of axon guidance. *rbr-2* is the sole nematode homolog of the human XLMR gene *JARID1C* (*KDM5C*), and controls axon guidance in a similar subset of neurons by reducing the expression of actin-related genes, including *wsp-1* (Mariani et al., 2016). The fact that *rbr-2* and *jmjd-1.2* share similar phenotypes when ablated, are both required during embryogenesis and bind H3K4me3 through their PHD domains, suggests that these histone demethylases might regulate axon guidance in a concerted manner. Indeed, we previously reported that *rbr-2; jmjd-1.2* double mutants show similar levels of PVQ defects as the single mutants (Mariani et al., 2016), confirming that *rbr-2* and *jmjd-1.2* act in a common pathway regulating axon guidance. Altogether, these findings confirm that epigenetic factors are essential for the correct execution of developmental processes, providing novel insights into how neuronal development is achieved.

In conclusion, our study reveals a novel function of *jmjd-1.2* in axon guidance and provides the first evidence that the Hh-like pathway, as conserved in *C. elegans*, contributes to the correct establishment of axon migration.

MATERIALS AND METHODS

Genetics and strains

C. elegans strains were cultured using standard growth conditions at 20°C on *Escherichia coli* OP50 (Brenner, 1974). Strains were as follows: wild-type Bristol: N2; *jmjd-1.2(tm3713)* IV; CX5334: *oyIs14[(P_{psra-6}::GFP)+lin-15(+)]* V; MU1085: *bwIs2[(P_{pf1p-1}::GFP)+(pRF4)rol-6(su1006)]*; OH4887: *otIs182[P_{pinx-18}::GFP]*; VH648: *hdIs26[Podr-2::CFP; Psra-6::DsRed2] III*; SK4013: *zdlIs13[P_{tph-1}::GFP]* IV; EG1285: *oxIs12[(P_{unc-47}::GFP)+lin-15(+)]* X; NW1100: *evIs82b[(P_{unc-129}::GFP)+ dpy-20(+)]* IV; LE309: *lqIs2 [P_{posm-6}::GFP+lin-15(+)]* X; *wrt-8(tm1585)* V; RB2308: *C29F3.5/clec-230(ok3131)* V; *asp-6(tm2213)* V; RB1999: *grl-7(ok2644)* V; RB2183: *grl-16(ok2959)* I; VC2627: *F54F11.2/nep-17(ok3251)* III; VC1333: *evl-20&cut-3(ok1819)/mln1 [mls14 dpy-20(e128)]* II; VC233: *gpn-1(ok377)* X; CB3687: *che-14(e1960)* I; ML514: *che-14(ok193)* I; *wsp-1(gm324)* IV; VC2053: *wip-1(ok2435)* III/hT2 [*bli-4(e937); let-?(q782); qIs48*] (I,III); VC898: *cdc-42(gk388)/mln1 [mls14; dpy-10(e128)]* II; RB860: *nck-1(ok694)* X; CF162: *mig-2(mu28)* X; VC2706: *wve-1(ok3308)* I/hT2 [*bli-4(e937); let-?(q782); qIs48*] (I,III); CB566: *unc-34(e566)* V. Double-mutant animals were generated by standard crossing procedure. For a complete list of the transgenic strains generated for this study, see Table S4.

Generation of *jmjd-1.2(KO)* by CRISPR/Cas9

We generated a null mutant for *jmjd-1.2* [here termed *jmjd-1.2(KO)*] by the co-CRISPR approach described by Ward (2015). To identify the deletions, the following oligonucleotides (5'-3') were used: *jmjd-1.2Fw*, ATGCT-GCGTCTCGTTTCTCT; *jmjd-1.2Rev1*, TCATGTCGCTCATTCAAGC; and *jmjd-1.2Rev2*, ACATCGATCCGATTCCTTTG. The resulting PCR products were purified and sequenced. The mutation used in this study is a deletion of 4019 bp, starting five nucleotides upstream the *jmjd-1.2* ATG (IV:4660991) and ending 82 nucleotides after the stop codon. Sequences (5'-3') of sgRNAs are: sgRNA1_Fw, TCTTGATCTACACATTCCAAATG-GA; sgRNA1_Rev, AAACCTCCATTTGGAATGTGTAGATC; sgRNA2_Fw, TCTTGAAATTAATAAGATCGG; and sgRNA2_Rev, AAACCC-GATCTTAATAGTAATTTTC. The *jmjd-1.2(KO)* allele is shown in Fig. S1B.

Generation of transgenic constructs

The *jmjd-1.2::GFP* construct, which includes a 4715 bp fragment containing 786 bp of promoter and the entire genetic locus of *jmjd-1.2*, has been described previously (Kleine-Kohlbrecher et al., 2010). Plasmids carrying the *jmjd-1.2* gene fused to *GFP* and under the control of specific promoters were constructed using the MultiSite Gateway Three-Fragment Vector Construction Kit (Life Technologies). The constructs used in Fig. 3B and Fig. 4B-D,F were generated as described in the supplementary Materials and Methods. The DNA sequences of all constructs were verified by sequencing.

Microinjection and production of transgenic lines

Transgenic lines were obtained through microinjection (Mello et al., 1991). Constructs were injected into young adult hermaphrodites as extrachromosomal arrays at 10–50 ng/μl with *Ptx-3::RFP* (50–90 ng/μl) or *Pmyo-2::mCherry* (0.5–5 ng/μl) as injection markers.

Fluorescence microscopy

For all transgenic markers, neuronal phenotypes were scored in L4 and young adult hermaphrodites grown at 25°C. Images were taken using an automated fluorescence microscope (Zeiss AXIO Imager M2) and Micro-Manager open source software (version 1.4.11). All pictures were exported using Photoshop (Adobe).

Dil staining of amphid and phasmid neurons

Staining was performed as described previously (Mariani et al., 2016).

Heat shock experiments

For overexpression experiments, embryos or L1 larvae were heat shocked at 37°C twice for 30 min each. After heat shock, worms were kept at 25°C overnight and L2/L3 larvae were analyzed by fluorescence microscopy the following day.

RNAi analysis

RNAi by feeding was carried out as described previously (Timmons et al., 2001). Constructs were obtained from the *C. elegans* RNAi Feeding Library (J. Ahringer's laboratory, Wellcome Trust/Cancer Research UK Gurdon Institute, University of Cambridge, Cambridge, UK) except for *ptc-1*, *ptc-3*, *tra-1* and *phg-1*, which were cloned into pCR2.1 TOPO vector using the TOPO TA Cloning Kit (Life Technologies). Empty L4440 vector was used as negative control. F2 progeny was analyzed for axon guidance defects at L4 stage. Three individual plates were scored for each variable, in three independent experiments. We observed a decreased percentage of defects in *jmjd-1.2(tm3713)* and wild-type animals treated with L4440 as compared with *jmjd-1.2(tm3713)* mutants (Table 3), suggesting that the phenotype measured is, for unclear reasons, sensitive to the bacterial strain used as a source of food. However, *jmjd-1.2(tm3713)* mutants treated with L4440 still have a significantly increased percentage of defects compared with wild-type animals grown under similar conditions ($P=0.0002$).

RNA-seq

Gravid hermaphrodites cultured at 25°C were treated with hypochlorite solution and embryos were flash-frozen in liquid nitrogen and stored at –80°C before RNA extraction. RNA was isolated from two independent cultures using TRIzol reagent (Life Technologies) and the RNeasy Mini Kit (Qiagen). RNA amplification and sequencing were performed by the Beijing Genomics Institute (BGI).

RNA-seq data analysis

Barcode and adaptor-cleaned sequences were checked for quality using FastQC (Babraham Bioinformatics) and mapped to the *C. elegans* genome (WS220) with TopHat 2.0.9 (Trapnell et al., 2012) using parameters described previously (Peltonen et al., 2013). Reads successfully mapped were >95% using a criterion of two mismatches. The number of reads processed and percentage aligned were: wild-type replicate 1, 43.2 M, 95.8%; wild-type replicate 2, 37.8 M, 96.0%; *jmjd-1.2* replicate 1, 39.9 M,

95.8%; *jmjd-1.2* replicate 2, 34.7 M, 95.9%. Mapped reads were analyzed for transcript assembly and differential expression using Cufflinks 2.1.1 (Trapnell et al., 2012) with a filter of 1.5-fold difference and FDR correction ($P < 0.05$). Differentially expressed genes were used for gene set enrichment analysis (GSEA) performed using DAVID 6.7 (Huang et al., 2009).

Real-time quantitative PCR (qPCR)

RNA isolation, cDNA synthesis and qPCR were performed as described previously (Mariani et al., 2016). The measures were normalized to *Y45F10D.4* (Zhang et al., 2012). All reactions were performed in duplicate, in two independent experiments.

Generation of antibody against JMJD-1.2

A polyclonal antibody against JMJD-1.2 was generated by Innovagen AB (IDEON Gamma Rec., Lund, Sweden), by immunizing rabbits with a purified bacterial GST-tagged fragment of the JMJD-1.2 protein encoded by the first four exons of the gene. The antibody was affinity purified and validated by western blot on lysate from mutant animals.

Western blot analysis

Whole-worm lysates for SDS-PAGE were prepared by boiling mixed-stage worms in SDS-PAGE loading buffer for 5 min. Protein concentration was estimated using the modified micro-Lowry assay. The following antibodies were used: rabbit polyclonal anti-JMJD-1.2 (Innovagen; 1:1000); mouse monoclonal anti-actin (Millipore, MAB1501; 1:15,000); peroxidase-labeled anti-rabbit and anti-mouse secondary antibodies (Vector Labs, PI-2000; 1:10,000).

Immunofluorescence

Whole worms were stained according to Finney and Ruvkun (1990). Primary antibody [polyclonal anti-JMJD-1.2 (Innovagen)] was incubated overnight at 4°C in a humid chamber and secondary antibody [donkey anti-rabbit IgG (Alexa Fluor 594, Invitrogen, A21207)] was incubated for 1 h at room temperature. Washes were in PBS/0.2% Tween 20. Vectashield H1200 mounting medium for fluorescence with DAPI was used to counterstain DNA.

Statistical analyses

All phenotypes were scored as percentages of defective animals among total observed. Statistical analyses were performed in GraphPad Prism 6 using Fisher's exact test for pairwise comparisons, or one-way ANOVA followed by Tukey's multiple comparison test for multiple comparisons. In rescue and overexpression experiments, significance was calculated in relation to non-transgenic controls for each transgenic line. As the penetrance of defects in non-transgenic siblings was always consistent with the phenotype of *jmjd-1.2(tm3713)*, these data are not shown in Fig. 2B,C, Fig. 3B and Fig. S3C. qPCR data were compared using Student's *t*-test. $P < 0.05$ was considered significant.

Acknowledgements

Some strains were provided by the CGC, which is funded by NIH Office of Research Infrastructure Programs (P40 OD010440). We thank the National BioResource project for *C. elegans* (Japan) and the international *C. elegans* Gene Knockout Consortium for providing strains; the Beijing Genomics Institute (BGI) for performing the RNA amplification and sequencing; Innovagen for generating the antibody against JMJD-1.2. We are grateful to Roger Pocock for strains and discussion and to Alexandra Avram, Andreea Talos and Line Kikarsen for technical assistance.

Competing interests

The authors declare no competing or financial interests.

Author contributions

A.R.R., L.M., E.M. and P.G.A. carried out the experimental work. J.P. and G.W. analyzed the RNA-seq data. A.R.S., L.M., E.M., P.G.A. and A.E.S. designed the experiments and analyzed the data. L.M. and A.E.S. wrote the manuscript.

Funding

This work was supported by the Danish National Research Foundation (Danmarks Grundforskningsfond; DNR82 to A.E.S.) and a University of Macau (Universidade de Macau) research grant (MYRG2015-00231-FHS to G.W.).

Data availability

RNA-seq data are available at the NCBI Sequence Read Archive (SRA) public database with the following accession numbers: BioProject, PRJNA354814; BioSample, SAMN06052359; Data, SRR5051663, SRR5051664, SRR5051665, SRR5051665.

Supplementary information

Supplementary information available online at <http://dev.biologists.org/lookup/doi/10.1242/dev.142695.supplemental>

References

- Abidi, F. E., Miano, M. G., Murray, J. C. and Schwartz, C. E. (2007). A novel mutation in the *PHF8* gene is associated with X-linked mental retardation with cleft lip/cleft palate. *Clin. Genet.* **72**, 19–22.
- Agha, Z., Iqbal, Z., Azam, M., Ayub, H., Vissers, L. E. L. M., Gilissen, C., Ali, S. H., Riaz, M., Veltman, J. A., Pfundt, R. et al. (2014). Exome sequencing identifies three novel candidate genes implicated in intellectual disability. *PLoS ONE* **9**, e112687.
- Asensio-Juan, E., Gallego, C. and Martínez-Balbás, M. A. (2012). The histone demethylase PHF8 is essential for cytoskeleton dynamics. *Nucleic Acids Res.* **40**, 9429–9440.
- Aspöck, G., Kagoshima, H., Niklaus, G. and Bürglin, T. R. (1999). *Caenorhabditis elegans* has scores of Hedgehog-related genes: sequence and expression analysis. *Genome Res.* **10**, 909–923.
- Aurelio, O., Hall, D. H. and Hobert, O. (2002). Immunoglobulin-domain proteins required for maintenance of ventral nerve cord organization. *Science* **295**, 686–690.
- Ayala, R., Shu, T. and Tsai, L.-H. (2007). Trekking across the brain: the journey of neuronal migration. *Cell* **128**, 29–43.
- Bénard, C. Y., Blanchette, C., Recio, J. and Hobert, O. (2012). The secreted immunoglobulin domain proteins ZIG-5 and ZIG-8 cooperate with L1CAM/SAX-7 to maintain nervous system integrity. *PLoS Genet.* **8**, e1002819.
- Bijlsma, M. F., Borensztajn, K. S., Roelink, H., Peppelenbosch, M. P. and Spek, C. A. (2007). Sonic hedgehog induces transcription-independent cytoskeletal rearrangement and migration regulated by arachidonate metabolites. *Cell. Signal.* **19**, 2596–2604.
- Bourikas, D., Pekarik, V., Baeriswyl, T., Grunditz, A., Sadhu, R., Nardó, M. and Stoeckli, E. T. (2005). Sonic hedgehog guides commissural axons along the longitudinal axis of the spinal cord. *Nat. Neurosci.* **8**, 297–304.
- Brenner, S. (1974). The genetics of *Caenorhabditis elegans*. *Genetics* **77**, 71–94.
- Bürglin, T. R. and Kuwabara, P. E. (2006). Homologs of the Hh signalling network in *C. elegans*. *WormBook* **28**, 1–14.
- Charron, F. and Tessier-Lavigne, M. (2005). Novel brain wiring functions for classical morphogens: a role as graded positional cues in axon guidance. *Development* **132**, 2251–2262.
- Chaudhry, A., Noor, A., Degagne, B., Baker, K., Bok, L. A., Brady, A. F., Chitayat, D., Chung, B. H., Cytrynbaum, C., Dymen, D. et al. (2015). Phenotypic spectrum associated with PTCHD1 deletions and truncating mutations includes intellectual disability and autism spectrum disorder. *Clin. Genet.* **88**, 224–233.
- Chia, P. H., Chen, B., Li, P., Rosen, M. K. and Shen, K. (2014). Local F-actin network links synapse formation and axon branching. *Cell* **156**, 208–220.
- Chiurazzi, P., Tabolacci, E. and Neri, G. (2004). X-linked mental retardation (XLMR): from clinical conditions to cloned genes. *Crit. Rev. Clin. Lab. Sci.* **41**, 117–158.
- Dent, E. W., Gupton, S. L. and Gertler, F. B. (2011). The growth cone cytoskeleton in axon outgrowth and guidance. *Cold Spring Harb. Perspect. Biol.* **3**, pii: a001800.
- Drickamer, K. and Dodd, R. B. (1999). C-Type lectin-like domains in *Caenorhabditis elegans*: predictions from the complete genome sequence. *Glycobiology* **9**, 1357–1369.
- Feng, W., Yonezawa, M., Ye, J., Jenuwein, T. and Grummt, I. (2010). PHF8 activates transcription of rRNA genes through H3K4me3 binding and H3K9me1/2 demethylation. *Nat. Struct. Mol. Biol.* **17**, 445–450.
- Filges, I., Röthlisberger, B., Blattner, A., Boesch, N., Demougin, P., Wenzel, F., Huber, A. R., Heinemann, K., Weber, P. and Miny, P. (2011). Deletion in Xp22.11: PTCHD1 is a candidate gene for X-linked intellectual disability with or without autism. *Clin. Genet.* **79**, 79–85.
- Finney, M. and Ruvkun, G. (1990). The *unc-86* gene product couples cell lineage and cell identity in *C. elegans*. *Cell* **63**, 895–905.
- Fortschegger, K. and Shiekhattar, R. (2011). Plant homeodomain fingers form a helping hand for transcription. *Epigenetics* **6**, 4–8.
- Fortschegger, K., de Graaf, P., Outchkourov, N. S., Van Schaik, F. M. A., Timmers, H. T. M. and Shiekhattar, R. (2010). PHF8 targets histone methylation and RNA polymerase II to activate transcription. *Mol. Cell. Biol.* **30**, 3286–3298.
- Gomez, T. M. and Letourneau, P. C. (2014). Actin dynamics in growth cone motility and navigation. *J. Neurochem.* **129**, 221–234.
- Guerrero, I. and Kornberg, T. B. (2014). Hedgehog and its circuitous journey from producing to target cells. *Semin. Cell Dev. Biol.* **33**, 52–62.

- Hammond, R., Blaess, S. and Abeliovich, A. (2009). Sonic hedgehog is a chemoattractant for midbrain dopaminergic axons. *PLoS ONE* **4**, e7007.
- Hao, L., Aspöck, G. and Bürglin, T. R. (2006a). The hedgehog-related gene *wrt-5* is essential for hypodermal development in *Caenorhabditis elegans*. *Dev. Biol.* **290**, 323-336.
- Hao, L., Johnsen, R., Lauter, G., Baillie, D. and Bürglin, T. R. (2006b). Comprehensive analysis of gene expression patterns of hedgehog-related genes. *BMC Genomics* **7**, 280.
- Huang, C., Xiang, Y., Wang, Y., Li, X., Xu, L., Zhu, Z., Zhang, T., Zhu, Q., Zhang, K., Jing, N. et al. (2010). Dual-specificity histone demethylase KIAA1718 (KDM7A) regulates neural differentiation through FGF4. *Cell Res.* **20**, 154-165.
- Huang da, W., Sherman, B. T. and Lempicki, R. A. (2009). Bioinformatics enrichment tools: paths toward the comprehensive functional analysis of large gene lists. *Nucleic Acids Res.* **37**, 1-13.
- Jarov, A., Williams, K. P., Ling, L. E., Kotliansky, V. E., Duband, J.-L. and Fournier-Thibault, C. (2003). A dual role for Sonic hedgehog in regulating adhesion and differentiation of neuroepithelial cells. *Dev. Biol.* **261**, 520-536.
- Jenkins, D. (2009). Hedgehog signalling: emerging evidence for non-canonical pathways. *Cell. Signal.* **21**, 1023-1034.
- Kalil, K. and Dent, E. W. (2005). Touch and go: guidance cues signal to the growth cone cytoskeleton. *Curr. Opin. Neurobiol.* **15**, 521-526.
- Kleine-Kohlbrecher, D., Christensen, J., Vandamme, J., Abarrategui, I., Bak, M., Tommerup, N., Shi, X., Gozani, O., Rappsilber, J., Salcini, A. E. et al. (2010). A functional link between the histone demethylase PHF8 and the transcription factor ZNF711 in X-linked mental retardation. *Mol. Cell* **38**, 165-178.
- Klose, R. J., Kallin, E. M. and Zhang, Y. (2006). JmjC-domain-containing proteins and histone demethylation. *Nat. Rev. Genet.* **7**, 715-727.
- Koivisto, A. M., Ala-Mello, S., Lemmelä, S., Komu, H. A., Rautio, J. and Järvelä, I. (2007). Screening of mutations in the PHF8 gene and identification of a novel mutation in a Finnish family with XLMR and cleft lip/cleft palate. *Clin. Genet.* **72**, 145-149.
- Kolotuev, I., Apaydin, A. and Labouesse, M. (2009). Secretion of Hedgehog-related peptides and WNT during *Caenorhabditis elegans* development. *Traffic* **10**, 803-810.
- Kuwabara, P. E., Lee, M. H., Schedl, T. and Jefferis, G. S. (2000). A *C. elegans* patched gene, *ptc-1*, functions in germ-line cytokinesis. *Genes Dev.* **14**, 1933-1944.
- Laumonier, F., Holbert, S., Ronce, N., Faravelli, F., Lenzner, S., Schwartz, C. E., Lespinasse, J., Van Esch, H., Lacombe, D., Goizet, C. et al. (2005). Mutations in PHF8 are associated with X linked mental retardation and cleft lip/cleft palate. *J. Med. Genet.* **42**, 780-786.
- Lin, H., Wang, Y., Wang, Y., Tian, F., Pu, P., Yu, Y., Mao, H., Yang, Y., Wang, P., Hu, L. et al. (2010). Coordinated regulation of active and repressive histone methylations by a dual-specificity histone demethylase *ceKDM7A* from *Caenorhabditis elegans*. *Cell Res.* **20**, 899-907.
- Liu, W., Tanasa, B., Tyurina, O. V., Zhou, T. Y., Gassmann, R., Liu, W. T., Ohgi, K. A., Benner, C., Garcia-Bassets, I., Aggarwal, A. K. et al. (2010). PHF8 mediates histone H4 lysine 20 demethylation events involved in cell cycle progression. *Nature* **466**, 508-512.
- Loenarz, C., Ge, W., Coleman, M. L., Rose, N. R., Cooper, C. D. O., Klose, R. J., Ratcliffe, P. J. and Schofield, C. J. (2010). PHF8, a gene associated with cleft lip/palate and mental retardation, encodes for an Nepsilon-dimethyl lysine demethylase. *Hum. Mol. Genet.* **19**, 217-222.
- Mariani, L., Lussi, Y. C., Vandamme, J., Riveiro, A. and Salcini, A. E. (2016). The H3K4me3/2 histone demethylase RBR-2 controls axon guidance by repressing the actin-remodeling gene *wsp-1*. *Development* **143**, 851-863.
- Mello, C. C., Kramer, J. M., Stinchcomb, D. and Ambros, V. (1991). Efficient gene transfer in *C. elegans*: extrachromosomal maintenance and integration of transforming sequences. *EMBO J.* **10**, 3959-3970.
- Noor, A., Whibley, A., Marshall, C. R., Gianakopoulos, P. J., Piton, A., Carson, A. R., Orlic-Milacic, M., Lionel, A. C., Sato, D., Pinto, D. et al. (2010). Disruption at the PTCHD1 Locus on Xp22.11 in Autism spectrum disorder and intellectual disability. *Sci. Transl. Med.* **2**, e49ra68.
- Peltonen, J., Aarnio, V., Heikkinen, L., Lakso, M. and Wong, G. (2013). Chronic ethanol exposure increases cytochrome P-450 and decreases activated in blocked unfolded protein response gene family transcripts in *Caenorhabditis elegans*. *J. Biochem. Mol. Toxicol.* **27**, 219-228.
- Pocock, R., Bénard, C. Y., Shapiro, L. and Hobert, O. (2008). Functional dissection of the *C. elegans* cell adhesion molecule SAX-7, a homologue of human L1. *Mol. Cell. Neurosci.* **37**, 56-68.
- Qi, H. H., Sarkissian, M., Hu, G.-Q., Wang, Z., Bhattacharjee, A., Gordon, D. B., Gonzales, M., Lan, F., Ongusaha, P. P., Huarte, M. et al. (2010). Histone H4K20/H3K9 demethylase PHF8 regulates zebrafish brain and craniofacial development. *Nature* **466**, 503-507.
- Qiu, J., Shi, G., Jia, Y., Li, J., Wu, M., Li, J., Dong, S. and Wong, J. (2010). The X-linked mental retardation gene PHF8 is a histone demethylase involved in neuronal differentiation. *Cell Res.* **20**, 908-918.
- Quinn, C. C. and Wadsworth, W. G. (2008). Axon guidance: asymmetric signaling orients polarized outgrowth. *Trends Cell Biol.* **18**, 597-603.
- Redin, C., Gérard, B., Lauer, J., Herenger, Y., Muller, J., Quartier, A., Masurel-Paulet, A., Willems, M., Lesca, G., El-Chehadeh, S. et al. (2014). Efficient strategy for the molecular diagnosis of intellectual disability using targeted high-throughput sequencing. *J. Med. Genet.* **51**, 724-736.
- Robichaux, M. A. and Cowan, C. W. (2014). Signaling mechanisms of axon guidance and early synaptogenesis. *Curr. Top. Behav. Neurosci.* **16**, 19-48.
- Ropers, H.-H. and Hamel, B. C. J. (2005). X-linked mental retardation. *Nat. Rev. Genet.* **6**, 46-57.
- Sánchez-Camacho, C. and Bovolenta, P. (2008). Autonomous and non-autonomous Shh signalling mediate the in vivo growth and guidance of mouse retinal ganglion cell axons. *Development* **135**, 3531-3541.
- Sapio, M. R., Hilliard, M. A., Cermola, M., Favre, R. and Bazzicalupo, P. (2005). The Zona Pellucida domain containing proteins, CUT-1, CUT-3 and CUT-5, play essential roles in the development of the larval alae in *Caenorhabditis elegans*. *Dev. Biol.* **282**, 231-245.
- Sasaki, N., Kurisu, J. and Kengaku, M. (2010). Sonic Hedgehog signaling regulates actin cytoskeleton via Tiam1-Rac1 cascade during spine formation. *Mol. Cell. Neurosci.* **45**, 335-344.
- Siderius, L. E., Hamel, B. C. J., van Bokhoven, H., de Jager, F., van den Helm, B., Kremer, H., Heineman-de Boer, J. A., Ropers, H.-H. and Mariman, E. C. M. (1999). X-linked mental retardation associated with cleft lip/palate maps to Xp11.3-q21.3. *Am. J. Med. Genet.* **85**, 216-220.
- Soloviev, A., Gallagher, J., Marnet, A. and Kuwabara, P. E. (2011). *C. elegans patched-3* is an essential gene implicated in osmoregulation and requiring an intact permease transporter domain. *Dev. Biol.* **351**, 242-253.
- Sulston, J. E. (1983). Neuronal cell lineages in the nematode *Caenorhabditis elegans*. *Cold Spring Harb. Symp. Quant. Biol.* **48**, 443-452.
- Timmons, L., Court, D. L. and Fire, A. (2001). Ingestion of bacterially expressed dsRNAs can produce specific and potent genetic interference in *Caenorhabditis elegans*. *Gene* **263**, 103-112.
- Trapnell, C., Roberts, A., Goff, L., Pertea, G., Kim, D., Kelley, D. R., Pimentel, H., Salzberg, S. L., Rinn, J. L. and Pachter, L. (2012). Differential gene and transcript expression analysis of RNA-seq experiments with TopHat and Cufflinks. *Nat. Protoc.* **7**, 562-578.
- Tsukada, Y., Ishitani, T. and Nakayama, K. I. (2010). KDM7 is a dual demethylase for histone H3 Lys 9 and Lys 27 and functions in brain development. *Genes Dev.* **24**, 432-437.
- Vandamme, J., Sidoli, S., Mariani, L., Friis, C., Christensen, J., Helin, K., Jensen, O. N. and Salcini, A. E. (2015). H3K23me2 is a new heterochromatic mark in *Caenorhabditis elegans*. *Nucleic Acids Res.* **43**, 9694-9710.
- Ward, J. D. (2015). Rapid and precise engineering of the *Caenorhabditis elegans* genome with lethal mutation co-conversion and inactivation of NHEJ repair. *Genetics* **199**, 363-377.
- Weinberg, P., Flames, N., Sawa, H., Garriga, G. and Hobert, O. (2013). The SWI/SNF chromatin remodeling complex selectively affects multiple aspects of serotonergic neuron differentiation. *Genetics* **194**, 189-198.
- White, J. G., Southgate, E., Thomson, J. N. and Brenner, S. (1986). The structure of the nervous system of the nematode *Caenorhabditis elegans*. *Philos. Trans. R. Soc. Lond. B Biol. Sci.* **314**, 1-340.
- Yam, P. T. and Charron, F. (2013). Signaling mechanisms of non-conventional axon guidance cues: the Shh, BMP and Wnt morphogens. *Curr. Opin. Neurobiol.* **23**, 965-973.
- Yam, P. T., Langlois, S. D., Morin, S. and Charron, F. (2009). Sonic Hedgehog guides axons through a noncanonical, Src-family-kinase-dependent signaling pathway. *Neuron* **62**, 349-362.
- Yang, Y., Hu, L., Wang, P., Hou, H., Lin, Y., Liu, Y., Li, Z., Gong, R., Feng, X., Zhou, L. et al. (2010). Structural insights into a dual-specificity histone demethylase *ceKDM7A* from *Caenorhabditis elegans*. *Cell Res.* **20**, 886-898.
- Zhang, Y., Chen, D., Smith, M. A., Zhang, B. and Pan, X. (2012). Selection of reliable reference genes in *Caenorhabditis elegans* for analysis of nanotoxicity. *PLoS ONE* **7**, e31849.
- Zheng, C., Karimzadegan, S., Chiang, V. and Chalfie, M. (2013). Histone methylation restrains the expression of subtype-specific genes during terminal neuronal differentiation in *Caenorhabditis elegans*. *PLoS Genet.* **9**, e1004017.
- Zugasti, O., Rajan, J. and Kuwabara, P. E. (2005). The function and expansion of the Patched- and Hedgehog-related homologs in *C. elegans*. *Genome Res.* **15**, 1402-1410.